Constraining the ^{40}K decay constant with ^{87}Rb-^{87}Sr – ^{40}K-^{40}Ca chronometer intercomparison

Maria O. Naumenko-Dèzes[1,3], Thomas F. Nägler[1], Klaus Mezger[1], Igor M. Villa[1,2]

[1] *Institut für Geologie, Universität Bern, Baltzerstrasse 3, 3012, Bern, Switzerland*
[2] *Centro Universitario Datazioni e Archeometria, Università di Milano Bicocca, Piazza della Scienza 4, 20126 Milano, Italy*

[3] *present address: University Nice Sophia Antipolis, Géoazur Laboratory, Sophia Antipolis, 250 rue A. Einstein, 06560 Valbonne, France* / corresponding author marie@geosphere.ch

Keywords: K-Ca dating, Rb-Sr dating, ^{40}K decay constant, geochronometers intercalibration, Phalaborwa

Abstract

A literature survey reveals that the K-Ar chronometer gives ages that are *ca.* 1 % younger than U-Pb ages. This offset is generally attributed to an inaccurate ^{40}K decay constant. Three geological samples selected from a shortlist of eight with known U-Pb ages were investigated using detailed petrological methods and subsequently the Rb-Sr and K-Ca chronometers in order (a) to evaluate if they meet the requirement of a geological "point-like" history (i.e. isochronic formation and subsequent ideal closure of chronometers) and (b) to narrow down the systematic uncertainty on the ^{40}K decay constant by investigating the metrologically traceable K-Ca decay branch. Lepidolite of the Rubikon pegmatite, Namibia, was dated with Rb-Sr at 504.7 ± 4.2 Ma and the phlogopite and apatite from the Phalaborwa carbonatite complex, South Africa, yielded a Rb-Sr age of 2058.9 ± 5.2 Ma. Both Rb-Sr ages agree with published U-Pb ages. The Rb-Sr age of the late Archean Siilinjärvi carbonatite, Finland, records a later regional metamorphic event at 1869 ± 10 Ma. Only the samples from the Phalaborwa complex represent a "point-like" magmatic event and meet all the criteria to make them suitable for the ^{40}K decay constant intercalibration. The Phalaborwa K-Ca isochron has a slope of 1.878 ± 0.012. Forcing the K-Ca isochron to coincide with the U-Pb and Rb-Sr ages gives one equation with two unknowns. Assuming that the branching ratio of the K-Ca branch, B_{Ca}, lies in the interval ($k = 2$) of all published references, $0.8925 < B_{Ca} < 0.8963$, then the most reliable uncertainty interval ($k = 2$) for the total ^{40}K decay constant, λ_{tot}, is calculated as $5.484 \times 10^{-10}\ a^{-1} < \lambda_{tot} < 5.498 \times 10^{-10}\ a^{-1}$. This confirms that the currently used IUGS recommendation is inaccurate.

1. Introduction

The branched decay of ^{40}K may provide two useful dating tools for K rich minerals based on the decay to ^{40}Ca and ^{40}Ar. However, multiple complications with the estimate of the decay constants have so far prevented obtaining an accuracy better than ca. 1 % on K-Ar ages (see Appendix 1). The widespread use of ^{40}K-^{40}Ca chronometer is hampered by the high amount of non-radiogenic Ca in most minerals, which in many cases does not allow precise dating. Both K dating systems depend on precise and accurate decay constants for ^{40}K: the decay constants of the Ca branch (λ_β), of the Ar branch (λ_{EC}), and the total decay constant ($\lambda_{tot} = \lambda_\beta + \lambda_{EC}$):

$$^{40}Ar^*/^{40}K = \lambda_{EC}/\lambda_{tot} \cdot [e^{(\lambda tot \cdot t)} - 1] \quad \text{Eq. 1}$$

$$^{40}Ca^*/^{40}K = \lambda_\beta/\lambda_{tot} \cdot [e^{(\lambda tot \cdot t)} - 1] \quad \text{Eq. 2,}$$

where the asterisk denotes the radiogenic daughter nuclides and t stands for time.

In the last two decades, there have been several attempts to re-evaluate the decay constants by physical and geochronological methods. The latter have been performed mostly by intercomparison of the K-Ar and U-Pb decay systems (e.g. Min et al., 2000; Kwon et al., 2002; Renne et al., 2010). When the ^{39}Ar-^{40}Ar method is used, experimenters must rely on irradiation monitors that themselves must be well-calibrated and have a "point-like" geological history. The calibration of the K-Ca branch is metrologically traceable, thus has less potential uncertainties and may provide useful data for the evaluation of K decay constants.

In recent decades, the uncertainty on the ^{40}K decay constant has been the limiting factor for the accuracy of K-Ar age determinations (and $^{40}Ar/^{39}Ar$ ages) and for the intercomparison of the K-Ar system with other decay systems. In the 40 years since the IUGS recommendation by Steiger and Jäger (1977) there have been numerous attempts to reduce the uncertainty, as reviewed by

Begemann et al. (2001). These authors pointed out that three different experimental approaches are *a priori* suitable for the determination of a decay constant: (1) counting of the radiation (α, β, γ) emitted by the decaying radioactive parents; (2) laboratory accumulation of the radioactive daughter products over a suitably long time; (3) geological intercomparison of samples of known age, with the essential proviso that the only suitable samples are those that have had a "point-like" geological history (Begemann et al., 2001), i.e. had a isochronic origin and were later unaffected by secondary processes (mineralogical, chemical, thermal, mechanical, etc.). In the case of the K-Ar decay system (Fig. 1), progress has been slower than for other nuclide pairs. The first difficulty is that the branched decay scheme of ^{40}K is subject to controversies to this day. The K-Ca branch only consists of a single β^- decay with a well-defined energy of 1.31 MeV, accompanied by the emission of γ rays with an energy ≤ 1.31 MeV. The K-Ar branch potentially consists of three transitions: (i) electron capture (EC) leading to an excited level of the daughter nucleus, ^{40}Ar, accompanied by the emission of γ rays with an energy ≤ 1.46 MeV; (ii) EC leading directly to the ground state of ^{40}Ar, without emission of γ rays; (iii) emission of a positron. The γ-rays from transition (i) can be, and have been, counted. Those from transition (iii) could be counted, but have not been observed so far, which has led the physics community to calculate its probability to be ≤ 10^{-5} (Bé et al., 2010). The γ-less transition (ii) cannot be counted. In their recent review, Mougeot and Helmer (2009) stated that theoretical calculations constrain it to be 0.02 ± 0.01 times transition (i). However, the very existence, and *a fortiori* the magnitude, of an unobservable transition has been questioned by Kwon et al. (2002).

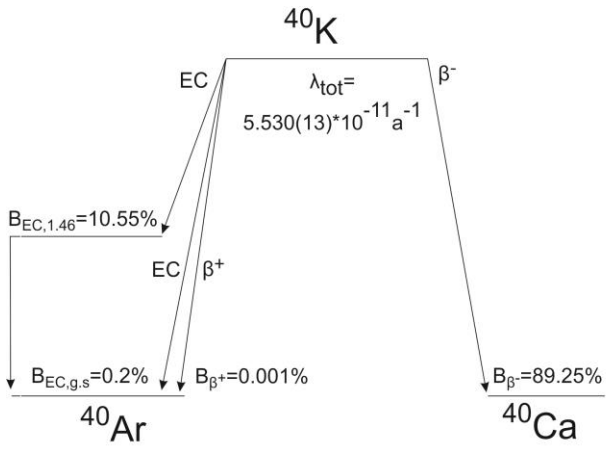

Fig.1. Decay scheme of ^{40}K after Bé et al. (2010), where $B_{EC,\ 1.46}$ is the electron capture branch with γ ray emission intensity of 1.46 MeV, $B_{EC,\ g.s.}$ is the "gammaless" electron capture branch to the ground state of ^{40}Ar, $B_{\beta+}$ and $B_{\beta-}$ are the $\beta^-$and β^+decay branches.

Kossert and Günther (2004) used liquid scintillation counting experiments to determine the total decay constant of ^{40}K. However, the experiment included the measurement of two very different radiation types: the β^- particles of the K-Ca branch and the γ rays of the K-Ar branch. Only the total counting efficiency of the scintillator was independently calibrated, but not the individual efficiencies. The data reduction thus amounted to solving two equations with three unknowns. Kossert and Günther (2004) proposed to assume a reasonable value for one of the unknowns, the branching ratio, so as to partition the corresponding detection efficiencies (0.998 for the β^- particles,

0.198 for the γ rays. In fact, by deconvolving the bulk count rates into two separate branches using the values given by Kossert and Günther (2004), it is possible to reconstruct the count rate of the β^- branch and to calculate from it the decay constant of the K-Ca branch, $\lambda\beta = (4.942 \pm 0.022) \times 10^{-10}$ a^{-1}. This still leaves open the question of the total decay constant.

Accumulation experiments can be performed with high precision, provided that the amounts of matter of parent and daughter isotopes can be metrologically traced. In the case of the ^{87}Sr accumulation experiment started by Davis et al. (1977) and concluded by Rotenberg et al. (2012), two factors contributed to its success: the comparatively large isotopic abundance of ^{87}Rb, ca. 27 % of the total element, and the ability to determine Sr concentrations in a traceable chain. For the ^{40}K decay to ^{40}Ar neither of these parameters is favorable. ^{40}K is a rare isotope with only ca. 0.01 % of the total element (Naumenko et al., 2013). Metrologically traceable Ar concentration measurements have so far never succeeded (Miiller, 2006; Morgan et al., 2011). In contrast, accumulation experiments for the K-Ca branch can be made traceable, but have not been attempted so far.

Geological intercalibrations involve much more than mass spectrometric analyses and their total uncertainty is not just the internal repeatability of the isotope measurement. Instead, they are subject to the requirement of a point-like geological history. To ensure that the uncertainty reaches the 1 % level it is necessary to ascertain that any possible artifact was smaller than 0.1 %. This requires a control on essential mineralogical aspects (such as stoichiometry) at the 99.9 ± 0.1 % level, which exceeds the present-day resolution of chemical microanalysis by at least one order of magnitude (the repeatability of major element analyses by electron probe microanalyzer (EPMA) is *ca*. 1 %). Since metrologically traceable Ar concentration measurements are not available, geological intercalibrations of the K-Ar decay not only require the identification of comparison samples with point-like geological histories; they also extend this requirement to the reference monitors (formerly incorrectly called "age standards") that are used as age calibrators. An external, *post-facto* assessment of the suitability of intercomparison samples from the literature is impossible without a characterization of exactly the same hand-specimen. But as these intercalibrations amount to just half a dozen of widely distributed monitor samples, it is sufficient to examine in detail how homogeneous and how reproducible these few crucial monitors are to assess all intercalibrations (Appendix 1).

2. Analytical methods

2.1. Sample selection criteria

The main criteria for sample selection were that samples should have a “point-like” geological history (Begemann et al., 2001), with all isotopic systems staying >> 99 % closed after formation. The necessary, but not sufficient, condition for it is that samples preserve their primary chemical composition. Any retrogression (which would violate the requirement of ideal isotopic closure after emplacement) results in easily diagnosed chemical disturbances. Spatial homogeneity of trace elements and their ratios is also a monitor of possible diffusive reequilibration (Villa, 2016). The necessity to demonstrate the absence of retrogression at the level of < 1% is a prerequisite to reduce the systematic uncertainty on geological intercalibration below 1 %.

The present study relies on the intercomparison of two chronometers, K-Ca and Rb-Sr, with the U-Pb age considered as a reliable anchor. The benefits of such double intercomparison are twofold. (i) As the solubility of K, Rb, Ca and Sr is normally quite high in HCl, it is possible to dissolve a mg-size fragment of the chosen minerals, split the solution, and analyze K-Ca and Rb-Sr systematics on exactly the same material (Gopalan and Kumar, 2008). (ii) The parent elements are both alkali metals, and the daughter elements are both alkaline earths (Shih et al., 1993). This ensures that closed behavior of a mineral relative to one pair of elements is extremely likely to correspond to closed behavior for the other pair.

The selected samples should be old enough to have accumulated a measurable quantity of radiogenic Ca. This makes sample choice problematic, as old rocks have had a higher chance of having been affected by chemical and thermal alteration than younger samples. Eight samples with known U-Pb ages and expected simple geological history were evaluated based on literature data, optical microscopy and electron microprobe data (EPMA) to exclude those with internal petrologic disequilibrium (Appendix 2). Three samples were chosen for the Rb-Sr and K-Ca age determination.

The Phalaborwa phoscorite comes from a well-studied carbonatite complex, located in north-eastern Transvaal, South Africa. It belongs to an intracratonic alkali intrusive complex composed mainly of clinopyroxenites with minor carbonatites and phoscorites. It intruded an Archean terrane of granites, gneisses, quartzites, amphibolites, talc and serpentine schists (Eriksson, 1984). The Phalaborwa complex has been dated in numerous studies (Table 1). Wu et al. (2011) dated different layers and found coincident ages for all of them, which conforms to the requirement that a sample records a "point-like" event. The carbonatite sample was also established by Nebel et al. (2011) as a reliable and accurate calibrator for the Rb-Sr decay constant by comparison with its U-Pb age. Our sample is a phoscorite (marked in this work as PhB-2) that consists of large crystals (up to 10 cm) of phlogopite (*ca*. 45%), apatite (*ca*. 35%), diopside (*ca*. 14%), ilmenite (*ca*. 5%) and calcite (*ca*. 1%). Apatite forms both large euhedral grains (up to 10 cm) and subhedral inclusions < 200 μm in phlogopite and diopside grains. Small (20-200 μm) ilmenite and calcite grains fill intergranular boundary spaces (Fig. 2.). Inclusions of apatite and calcite make it difficult to achieve highly radiogenic values of ^{40}Ca. Signs of serpentinisation along diopside cleavage planes can be observed. Phlogopite appears visually to be pristine. The homogeneity of phlogopite was confirmed with element maps and quantitative major element profiles by EPMA (see Appendix 2). No signs of alteration or zonation of phlogopite was found at the resolution of the electron microprobe, viz. relative concentration uncertainties of ca. 1-2 % for major elements and spatial resolution of ca. 2-3 μm.

The second sample is a lepidolite from the Rubikon mine, located within the Karibib pegmatite belt, Namibia. The Rubikon pegmatites intruded into medium- to high-grade metamorphic rocks within a quartz monzonite of Neoproterozoic age (700 – 500 Ma), and a pegmatitic granite of Ordovician-Cambrian age (600 – 460 Ma). Columbite from the Rubikon pegmatite has been dated by U-Pb thermal ionization mass spectrometry (TIMS) at 505.5 ± 2.6 Ma (Melcher et al., 2015). The lepidolite sample (Lep) consists of large pristine pink sheets, that can be easily sliced with a blade into thin transparent pieces along their cleavage planes. The EPMA shows that the sheets have no inclusions of other minerals resolvable from noise, no zonation or signs of

alteration (see Appendix 2). Element maps show uniform distribution of Al, F, K, Mn and Rb. Quantitative profile analysis also confirms homogeneity of the sample within the uncertainty of the microprobe. Very high K (ca. 80000 ppm) and Rb (*ca.*11200 ppm) concentrations make this sample a good candidate for simultaneous dating with the Rb-Sr and K-Ca methods.

The third sample is a phlogopite from the Siilinjärvi carbonatite complex in the Karelian Craton (Finnland) within the Ladoga-Bothnian deep fracture zone. The *in situ* Pb-Pb zircon age of the intrusion of the complex is 2594 ± 13 Ma (Rukhlov and Bell, 2010). The sample (Si-102) consists of a calcite matrix (*ca*. 80 %) with apatite (*ca.* 10 %), phlogopite (*ca.* 10 %) and magnetite (< 1 %). Calcite grains are anhedral and up to 1 mm large, apatite grains are *ca.* 2 mm large with rounded edges and multiple inclusions of small (*ca.* 1-10 μm) grains of calcite and phlogopite. The mica occurs as up to 5 mm long sheets, that show irregular fading in cross-polarized light, pristine look in thin-sections (Fig. 3) and the homogeneity of the mica sheets has been confirmed with element mapping using EPMA (see Appendix 2).

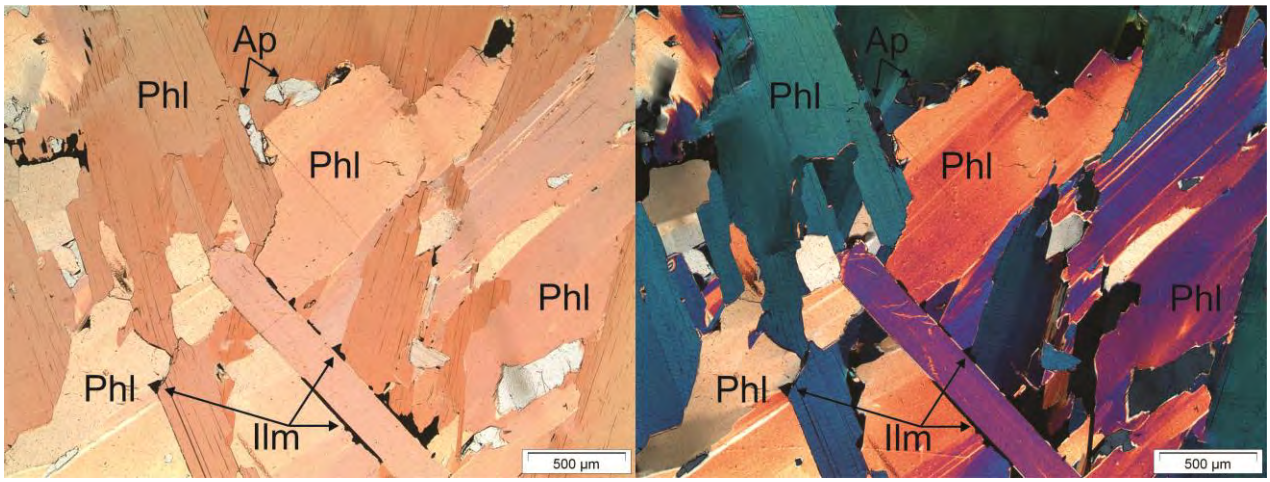

Fig 2. Phalaborwa phoscorite thin section: left, plane-polarized light; right, cross-polarized light.

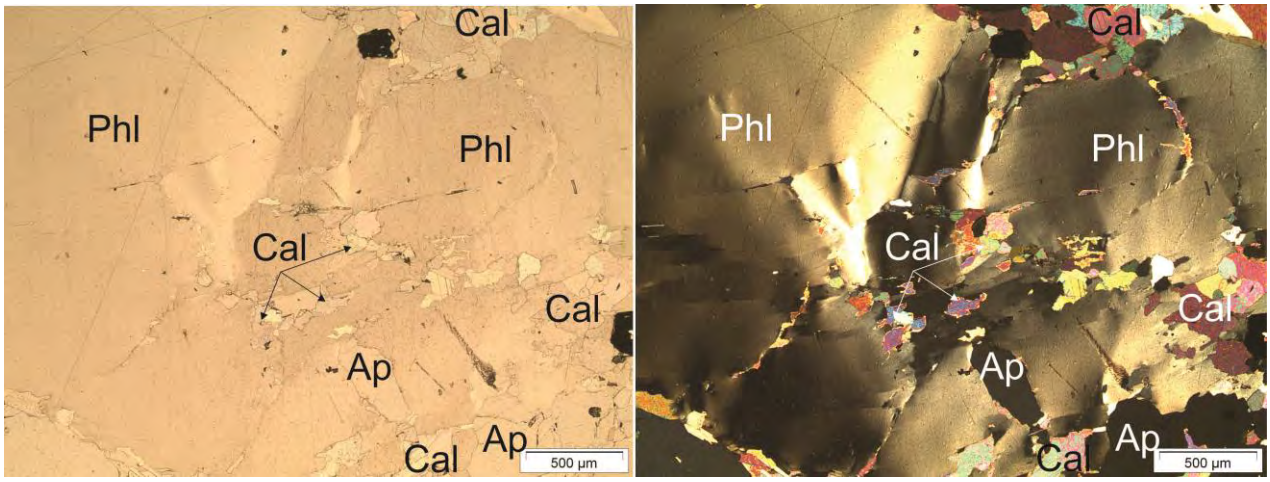

Fig. 3. Thin section of the Siilinjärvi carbonatite: left, plane-polarized light, right, cross-polarized light.

189 Table 1. Ages for the Phalaborwa complex from the literature.

190 * Rb-Sr age recalculated to $\lambda_{87} = 1.3972 \times 10^{-11}\ a^{-1}$ (Villa et al., 2015) replacing the λ_{87} in the original papers; for
191 Eriksson (1984) it was assumed that the ^{87}Rb decay constant of Steiger and Jäger (1977) was used originally.

Age (Ma)	Method	Mineral	Rock type	Reference
2060	U-Pb	uranothorianite		Holmes and Cahen (1956)
2047 ± 19*	Rb-Sr	phlogopite	clinopyroxenite, carbonatite and phoscorite	Eriksson (1984)
2047 +11 / -8	U-Pb	thorianite and baddeleyite	carbonatite and phoscorite	Eriksson (1984)
2059.8 ± 0.8	U-Pb	baddeleyite	carbonatite	Heaman and LeCheminant (1993)
2060.6 ± 0.5	U-Pb	baddeleyite		Reischmann (1995)
2057 ± 8	U-Pb	baddeleyite	not indicated	Horn et al. (2000)
2057.1 ± 2.6	U-Pb	baddeleyite	not indicated	Wingate and Compston (2000)
2059.6 ± 0.4	U-Pb	baddeleyite	carbonatite	French et al. (2002)
2026 +46 / -47	chemical U–Th–total Pb	baddeleyite	carbonatite	French et al. (2002)
2095±74*	Rb-Sr	hornblende, felsic fraction, clinopyroxene	dolerite	Yuhara et al. (2005)
2045±93*	Rb-Sr	whole rock and mineral	phoscorite	Yuhara et al. (2005)
2050.2 ± 4.8*	Rb-Sr	phlogopite, appatite	carbonatite	Nebel et al. (2011)
2060.1±4.1 2050±13	U-Pb (in situ)	baddeleyite zircon	outer pegmatitic pyroxenite of Loolekop pipe	Wu et al. (2011)
2061.7±2.4 2047±27	U-Pb (in situ)	baddeleyite zircon	main phoscorite	Wu et al. (2011)
2060.0±2.2	U-Pb (in situ)	baddeleyite	banded carbonatite	Wu et al. (2011)
2056.7±2.7 2059.8±1.3 2053±14	U-Pb (in situ)	baddeleyite baddeleyite zircon	transgressive carbonatite	Wu et al. (2011)
2068±17 2049±28	U-Pb (in situ)	baddeleyite zircon	satellite syenite (plug-like bodies outside the border of main complex)	Wu et al. (2011)
2035±35	U-Pb (in situ)	baddeleyite	later mafic dyke	Wu et al. (2011)
2060.3±0.4	Pb-Pb	baddeleyite	carbonatite	Kumar et al. (2014)

192

193

2.2. Sample preparation

Phlogopite, apatite and calcite were detached from the hand specimen with a steel scalpel (pre-cleaned with distilled water) into a Petri dish. Sheets of phlogopite were disconnected from each other to obtain as thin and transparent sheets as possible. Earlier attempts to remove apatite by grinding the mica sheets resulted in high and variable Ca contamination (e.g. PhB2c2d in Table 3) and therefore this procedure was discontinued. Transparent mica flakes were hand-picked under a binocular microscope to ensure visually that no other minerals are present in the mica fraction, though apatite or calcite inclusions < 1 μm are undetectable by this technique. The hand-picked minerals were ultrasonically cleaned from adhering dust in distilled water. The samples were dried at 50 °C overnight and then weighed. *Circa* 5 mg of phlogopite and 30 mg of lepidolite were used for dating. Most of the samples were spiked before dissolution and in case of dividing the sample into aliquots for different dating methods, the K-Ca and Rb-Sr aliquots were spiked separately, due to the presence of Sr in the K-Ca mixed spike (the presence of ^{86}Sr in ^{43}Ca spike was also previously reported by Baadsgaard (1987) and Gopalan (2008)). The Rb-Sr spike calibrated in the University of Münster, Germany, had the following composition: $^{86}Sr/^{84}Sr = 0.04341$, $^{87}Sr/^{84}Sr = 0.01991$, $^{88}Sr/^{84}Sr = 0.17351$, $^{85}Rb/^{87}Rb = 0.020408$, $^{84}Sr/^{87}Rb = 0.002171$, K-Ca spike described below.

Three different procedures were applied to obtain K and Ca for analysis: (1) dissolution in HF and HNO_3 on a hot plate at 100 °C for two weeks; (2) leaching in aqua regia at 100 °C for two weeks (Villa et al., 2006); (3) leaching with HCl and HNO_3 for one week, pipetting off the supernatant, dissolution of the residue with HF + HNO_3 on a hot plate at 100 °C for a few days, evaporating, finally recombining the leachate and the dissolved residue (Nägler and Kamber, 1996) (a detailed description of K-Ca sample dissolution procedures is given in Appendix 3). Dissolution and leaching on a hot plate was performed in screw-top Teflon® beakers. All samples were finally converted into chlorides with 6.4M HCl, evaporated and dissolved in 2.5 M HCl for column chemistry. The results of all three procedures plot on the same isochron for Phalaborwa phlogopite, however the third one was often found to be contaminated with a random amount of Ca that might come with dust particles during handling. Therefore, procedure (2) is preferable for small amounts of mica. The K-Ca column chemistry followed Nägler and Villa (2000) and was performed with 300 μl Teflon® columns custom made from heat shrink Teflon® tubing. The columns were filled with Dowex AG 50WX8 resin. K-Ca columns and resin were pre-cleaned with triple distilled acids: 3 cycles of 3 mL each of 2.5M HCl – 6.4M HCl – 2.5M HCl – Milli-Q™ water, followed by 1 mL of 1M ammonium acetate and 3 mL of Milli-Q™ water, to reach column blanks of < 0.5 ng. The total procedure blank for Ca was *ca.* 1 ng and was monitored on a routine basis. Triple distilled acids were used for K-Ca separation and single distilled for Rb-Sr. The Rb-Sr columns of 6.5 mm diameter were filled with 6 ml of Dowex AG 50WX8 resin. Rb and Sr were eluted with distilled 2.5 M HCl. The Sr fraction was later purified with Sr•Spec® resin (Horwitz et al., 1992). The total procedure blank for Sr was *ca.* 150 pg and was monitored on a routine basis.

2.3. Measurements

The isotope abundances of Ca, K and Sr were measured at the Institut für Geologie, University of Bern (Switzerland) on a ThermoScientific Triton Plus® multicollector TIMS equipped with a Faraday collector array specially designed for static Ca isotope measurements (covering

masses 40 to 48). The detailed description of the Ca measurement protocol is given by Naumenko-Dèzes et al. (2015). The Ca isotopes 42 to 48 were measured on Faraday cups connected to 10^{12} Ω resistors; ^{40}Ca was measured on a Faraday cup connected to a 10^{11} Ω resistor. Resistors used for ^{39}K and ^{41}K were 10^{11} Ω and those used for ^{40}K were 10^{12} Ω. Strontium isotopes were measured using exclusively 10^{11} Ω resistors. Amplifier gain calibration was performed on a daily basis using the built-in stable tension source of 3 V. A detailed discussion on the gain calibration and on the strong signal tail of ^{39}K can be found in Naumenko et al. (2013). Rubidium was measured on a Nu Instruments multicollector ICP-MS with a sample-bracketing protocol based on an in-house Rb reference solution and IUPAC Rb isotopic composition (de Laeter et al., 2003). The uncertainty of 0.2% on the Rb ratio was used for age calculations.

All data were corrected offline for instrumental mass fractionation (Appendix 3). During TIMS Ca measurements, the exponential fractionation factor ranged from -1 to +0.8; that for Sr from -0.45 to 0.53; that for K from -0.39 to 0.63. For ICP-MS Rb measurements it ranged from - 1.83 to - 1.67, being stable over a measurement day. A iterative double spike calculation was used for Ca isotope fractionation correction as the spike contains enriched ^{43}Ca and ^{48}Ca. A standard single-spike iteration calculation was used for Sr isotopic compositions. The K sample-spike mixtures were fractionation corrected following Chu et al. (2011) adapted for K. Isochrons were calculated with Isoplot 3.75 (Ludwig, 2012).

Uncertainties for Rb-Sr and K-Ca ages are presented as 2 standard errors (2SE), those for isotope ratios as 2 standard deviations (2SD). The uncertainty propagation for ages included the internal uncertainty of individual isotope ratio measurements, the spike uncertainty (on ratios and concentrations) and an error magnification for ^{40}K/^{44}Ca and ^{87}Rb/^{86}Sr based on the spike to sample ratio. The external reproducibility of the ^{40}Ca/^{44}Ca ratio was monitored with the NIST SRM 915b standard reference material during the sample acquisition period of seven months. We obtained 47.152 ± 16 (± 0.04% 2SD), exponentially corrected to ^{42}Ca/^{44}Ca =0.31221. The external reproducibility of Sr was monitored with NIST SRM 987 and resulted in 0.71038 ± 3 (± 0.004% 2SD), which is identical to the certified value. The weighing uncertainty for very small sample sizes (m < 0.01 g) was over 10 % in some cases, thus the concentration calculations for the samples in Tables 2-7 may differ from EPMA results or typical values for micas. However, this bias did not affect either the ^{40}K/^{44}Ca and ^{87}Rb/^{86}Sr ratios or the ages, since mixed spikes were added prior to the dissolution.

2.4. K-Ca mixed spike calibration

The K-Ca mixed spike was prepared from an enriched ^{40}K spike (relative abundances ^{39}K = 62.0 %, ^{40}K = 34.95 %, ^{41}K = 3.05 %) and a ^{43}Ca-^{48}Ca double spike (relative abundances ^{40}Ca = 6.55 %, ^{42}Ca = 0.43 %, ^{43}Ca = 42.05 %, ^{44}Ca = 2.56 %, ^{46}Ca < 0.01 %, ^{48}Ca = 48.41 %). The rationale, and the mathematics, of double spiking was established by Russell et al. (1978). In order to solve the equations, it has become customary to use an iterative spreadsheet (whose flowchart is given, e.g., by Heuser et al. (2002)). The isotopic composition of the K spike was measured with the total evaporation technique with an in-run precision of ± 0.30 % (2SE) for ^{40}K/^{41}K and ± 0.12% (2SE) for ^{39}K/^{41}K. No additional fractionation correction was applied to the K fraction of the K-Ca mixed spike. As a first approximation, the Ca isotopic composition of the spike was measured with the total evaporation technique. The resulting values were refined applying the iterative

fractionation calculation in Heuser et al. (2002) based on three different spike-standard mixtures using values of Russel et al. (1978) as Ca natural composition. Following these procedures, an uncertainty of <0.2 % (2σ) on the $^{40}Ca/^{44}Ca$, $^{43}Ca/^{44}Ca$ and $^{48}Ca/^{44}Ca$ ratios of the K-Ca mixed spike was achieved.

The element concentration of the K-Ca mixed spike was calibrated with two mixtures of NIST standards (NIST SRM 3109a, NIST SRM 3141a) and custom ordered mixed standards traceable to NIST (Certipur® 1.70342.0100, Certipur® 1.70308.0100). Three mixtures for each NIST and Certipur® standards were prepared in screw-top PTFE beakers. Each weighing step was performed five to six times to ensure that there were no weighing artifacts. The repeatability of weighing was better than 0.02 %, and was propagated into the concentration uncertainties. Due to the high Ca concentration of the original standard mixtures, they were diluted. The uncertainty on the weighing (0.2 % for dilute NIST SRM 3109a) is also propagated into the total uncertainty calculation.

Potassium and Ca of the standard-spike mixtures were separated on the same K-Ca columns and measured following the same procedure as for the samples. The procedure was repeated several times for each mixture to monitor laboratory contamination. Column blanks were below 1 ng, but some Ca fractions suffered from random contamination, which shifted the resulting Ca spike concentration downwards. Such erratic results were eliminated. Due to the high K concentration in the sample-spike mixtures the calculated K concentrations were not affected by contamination.

The summary of 36 measurements of six spike-standard mixtures for Ca yielded $^{40}Ca/^{44}Ca = 3.7807$, $^{42}Ca/^{44}Ca = 0.1672$, $^{43}Ca/^{44}Ca = 15.9574$, $^{48}Ca/^{44}Ca = 18.3943$, $^{43}Ca/^{48}Ca = 0.86752$, $^{40}K/^{41}K = 11.456$, $^{39}K/^{41}K = 20.325$, $^{43}Ca/^{40}K=0.39501$ with 0.5 ‰ repeatability of results. Thus, the uncertainty of NIST standards was the dominant source of uncertainty for the K-Ca mixed spike concentrations. The propagation of weighing repeatability, measurement uncertainty and NIST standard concentration uncertainty resulted in a total uncertainty of 0.17 % for Ca and 0.29 % for K concentrations at the 95 % confidence level.

The repeatability of the $^{40}Ca/^{44}Ca$ ratio using mixed spike was tested on four spike-standard (Certipur® 1.70342.0100) mixtures. The mixtures were put through sixteen K-Ca columns. 265 measurements resulted in spike corrected $^{40}Ca/^{44}Ca$ ratio of 47.151±0.028 (2SD), which is identical to unspiked measurements on this standard (47.154 ± 0.030 (2SD)) (unspiked results exponentially corrected for fractionation to $^{42}Ca/^{44}Ca=0.31221$ (Russell et al, 1978)).

3. Results

Rb-Sr dating of the Phalaborwa phlogopite was performed on nine phlogopite fragments and one apatite. The resulting Rb-Sr age was 2058.9 ± 5.2 Ma (Table 2, Fig. 4a). One phlogopite fragment was rejected due to an anomalously low Rb content. The concordance of the Rb-Sr age with the literature U-Pb age (2060.3 ± 0.4 Ma, Table 1) establishes the suitability of this Phalaborwa sample for accurate calibration. K-Ca dating was performed on twelve phlogopite fragments and four apatite grains of different weight and one calcite. Some phlogopite samples were divided into aliquots after dissolution. The solution aliquots were used either for multi-method dating (Rb-Sr

and K-Ca) or for repeatability tests (one solution divided among several columns in parallel, each eluate analyzed separately, as indicated in Table 3). The apatite was analyzed unspiked, assuming zero K and Rb content. The spread of points along the isochron (Fig. 4b) is most probably due to sub-microscopic apatite inclusions in phlogopite. The calculated K concentrations coincide with those measured with EPMA. The K-Ca isochron has a slope of 1.878 ± 0.012 (2σ). Using the decay constants of Steiger and Jäger (1977), this slope corresponds to an age of 2040.0 ± 13.0 Ma (2σ).

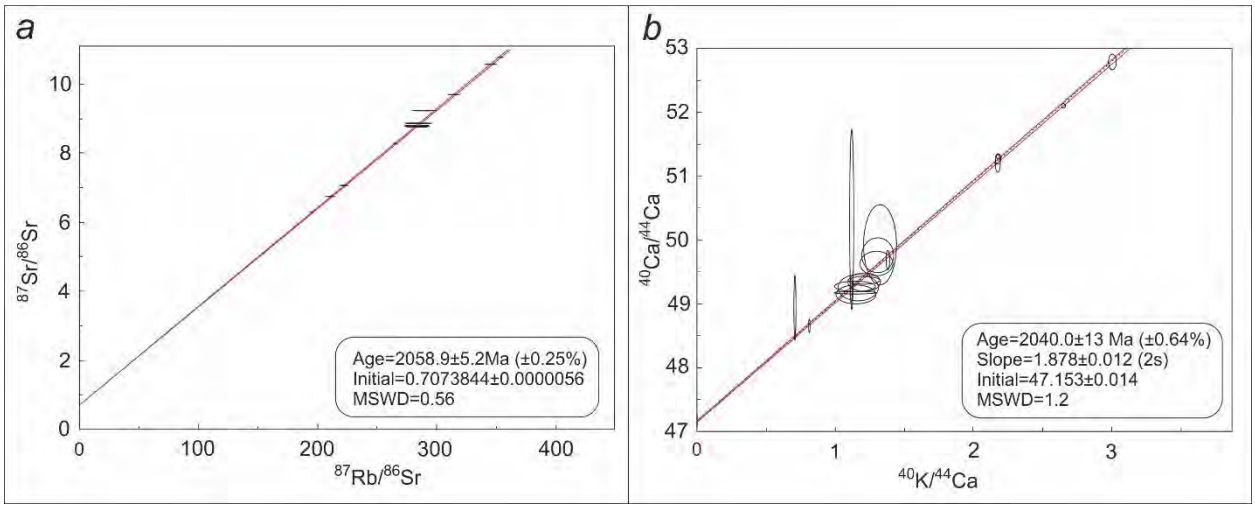

Fig. 4. Isochron diagrams for Phalaborwa phoscorite (PhB-2). (*a*) Rb-Sr isochron for 9 phlogopite fragments and one apatite grain calculated with a decay constant $\lambda_{87} = (1.3972 \pm 0.0045) \times 10^{-11}\ a^{-1}$ (Villa et al., 2015). (*b*) K-Ca isochron for 12 phlogopite and four apatite fragments and one calcite defining a slope of 1.878 ± 0.012, which corresponds to an age of 2040 ± 13 Ma applying constants of Steiger and Jäger (1977).

Table 2. Rb-Sr results for Phalaborwa phoscorite sample. All uncertainties are given as 2 SE in-run uncertainty only.

Sample	Mineral	Mass (g)	$^{87}Sr/^{86}Sr$	2 SE	$^{87}Rb/^{86}Sr$	2 SE	Sr ppm	Rb ppm	Comments
PhB2c11	phlogopite	0.0347	9.2145	0.0026	282.6	8.6	11	563	Sample solution split on three columns.
PhB2c12		0.0347	8.8363	0.0021	277.7	8.5	11	563	
PhB2c13		0.0347	8.764	0.024	276.2	8.5	11	566	
PhB262	phlogopite	0.0162	6.25920	0.00003	190.0	1.1	15	651	
PhB26b	phlogopite	0.0195	5.07031	0.00002	149.8	1.0	17	611	
PhB281s	phlogopite	0.00666	8.26288	0.00013	259.1	1.5	12	624	
PhB282s	phlogopite	0.00679	10.75998	0.00016	345.1	2.0	11	650	
PhB2101	phlogopite	0.03652	6.71800	0.00056	205.6	3.0	15	676	Sample solution divided in two aliquots for Rb-Sr and K-Ca dating. Rb-Sr fraction split on four columns.
PhB2102	phlogopite	0.03027	7.0369	0.0018	216.5	2.6	15	670	
PhB2103	phlogopite	0.03115	9.67556	0.00089	306.7	3.8	12	691	
PhB2104	phlogopite	0.03589	10.5564	0.0012	337.1	3.7	9	539	
PhB28Ap	apatite	0.00442	0.7073901	0.0000002					Not spiked.

Table 3. K-Ca results for Phalaborwa phoscorite sample. A1, A2, B1, B2, C1 or C2 at the end of a sample name indicate a column through which an aliquot was run; if not stated the sample was run just through one column. All uncertainties are given as 2 SE in-run uncertainty only. All points are included in the isochron (Fig. 4b).

Sample	Mineral	Mass (g)	$^{40}Ca/^{44}Ca$	2 SE	$^{40}K/^{44}Ca$	2 SE	Ca ppm	K ppm	Comments
PhB2b10A1	phlogopite	0.009	51.184	0.107	2.175	0.015	259	89433	Sample solution split on three columns
PhB2b10B1			51.271	0.069	2.178	0.015	259	89308	
PhB2b10C1			51.299	0.027	2.185	0.015	258	89433	
PhB2c2d1A1	phlogopite	0.247	49.275	0.065	1.143	0.118	449	84601	Repeated measurements of the same column
PhB2c2d1A2			49.252	0.164	1.164	0.122	445	85386	
PhB2c2d1B1			49.148	0.119	1.15	0.119	447	84814	Same sample as 2d1A above, on a different column
PhB2c2d2A2	phlogopite	0.2445	49.367	0.051	1.205	0.091	443	87755	Sample solution split on four columns
PhB2c2d2B2			49.755	0.225	1.308	0.095	277	59162	
PhB2c2d2C1			49.632	0.157	1.301	0.096	404	85952	
PhB2c2d2C2			49.932	0.514	1.323	0.099	405	87094	
PhB2c2d3B1	phlogopite	0.2422	49.344	0.124	1.212	0.089	433	86407	
PhB2c2d4B2	phlogopite	0.2473	49.171	0.018	1.135	0.118	467	87446	
PhB91	phlogopite	0.0405	49.692	0.12	1.381	0.01	388	87619	
PhB92	phlogopite	0.0329	52.792	0.099	3.003	0.022	181	83869	
PhB101aliq	phlogopite	0.0365	48.658	0.084	0.813	0.006	387	85173	Solution divided in two aliquots for Rb-Sr and K-Ca dating. K-Ca fraction split on four columns.
PhB102aliq	phlogopite	0.0303	48.944	0.415	0.708	0.006	444	84778	
PhB103aliq	phlogopite	0.0312	49.205	0.154	1.117	0.008	279	83523	
PhB104aliq	phlogopite	0.0359	50.322	1.168	1.12	0.012	326	95631	
PhB105	phlogopite	0.0052	52.102	0.030	2.649	0.013	214	88605	
PhB27tr	calcite	0.0045	47.163	0.084	0.0000007	0.0000006	369780	456	
PhB27ap1	apatite	0.0493	47.163	0.084	0.0000005	0.0000005	398468	37	
PhB27ap2	apatite	0.0491	47.133	0.035	0.0000003	0.0000002	336648	18	
PhB25ap	apatite	0.0217	47.153	0.060	0.0000008	0.0000006	150468	21	
PhB28Ap3c	apatite		47.157	0.018					Not spiked.

Rb-Sr dating of four fragments of the Rubikon lepidolite resulted in an age of 504.7 ± 4.2 Ma (Fig. 5a, Table 4). Due to the highly radiogenic $^{87}Sr/^{86}Sr$ ratios (i.e. > 500), any choice of the initial Sr in the range 0.70 - 0.72 does not affect the resulting age significantly. The initial $^{87}Sr/^{86}Sr$ ratio was fixed here at 0.710. The Rb-Sr age agrees with the published U-Pb age of columbite, 505.5 ± 2.6 Ma (Melcher et al., 2015), implying that the lepidolite behaved as a closed system since its formation. The K-Ca dating resulted in an unacceptably high non-analytical dispersion (MSWD = 60) (Fig. 5b, Table 5). Green points in Fig. 5b represent a mica sample leached in aqua regia, then divided into eight solution aliquots that were run through different columns. The points lie along the mixing line between a radiogenic end-member (presumably the purest lepidolite) and blank. The isochron formed by the eight leached sample aliquots gives an age of 481.4 ± 3.3 Ma (MSWD=0.04) with the decay constants of Steiger and Jäger (1977) (Fig. 5c).

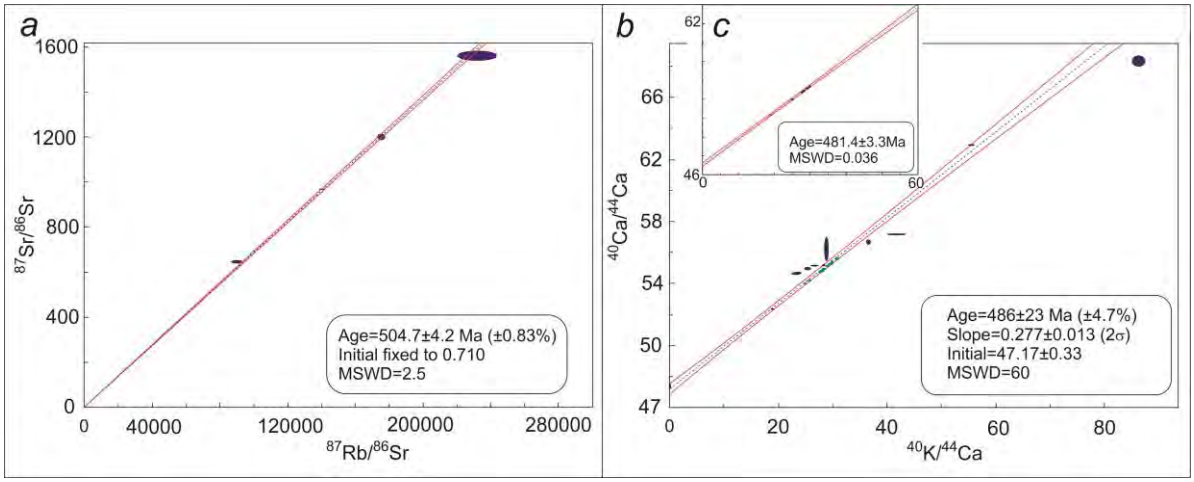

Fig. 5. Isochron diagrams for the Rubikon lepidolite: (*a*) Rb-Sr isochron for four lepidolite chips. The initial was fixed to 0.710. The age is calculated with a decay constant $\lambda_{87} = (1.3972 \pm 0.0045) \times 10^{-11}$ a^{-1} (Villa et al., 2015). *(b)* K-Ca regression with MSWD = 60. The corresponding dispersion is not acceptable. *(c)* K-Ca isochron of the lepidolite samples that were not treated with HF. The systematic deviations are much smaller (MSWD = 0.036) and the corresponding age calculated with constants of Steiger and Jäger (1977) is 481.4±3.3 Ma.

Table 4. Rb-Sr results for the Rubikon lepidolite. All uncertainties are given as 2 SE in-run uncertainty only.

Sample	Mineral	Mass (g)	$^{87}Sr/^{86}Sr$	2 SE	$^{87}Rb/^{86}Sr$	2 SE	Sr ppm	Rb ppm
Lep6	lepidolite	0.1070	640.8	8.3	86928	2608	18	8607
Lep81s	lepidolite	0.02577	966.7	2.2	136720	1367	23	11271
Lep82s	lepidolite	0.03047	1200.2	20.5	170372	1704	23	11241
Lep83s	lepidolite	0.02715	1562.7	32.0	225605	9024	22	11244

Table 5. K-Ca results for the Rubikon lepidolite. A1, A2, B1, B2, C1, C2 or D at the end of a sample name indicate a column through which a solution aliquot was run; if not stated the sample was run just though one column. All uncertainties are given as 2 SE in-run uncertainty only.

Sample	Mineral	Mass (g)	$^{40}Ca/^{44}Ca$	2 SE	$^{40}K/^{44}Ca$	2 SE	Ca ppm	K ppm	Comments
Lep2wA1	lepidolite	0.1024	54.958	0.022	25.39	0.42	20	74402	Sample solution split on 2 columns.
Lep2wA2		0.1024	55.142	0.009	26.67	0.44	19	75235	
Lep3eB1	lepidolite	0.0965	54.661	0.012	23.49	0.59	19	66639	Sample solution split on 2 columns.
Lep3eB2		0.0965	54.607	0.016	23.20	0.58	19	65929	
Lep5	lepidolite	0.01469	62.923	0.021	55.36	0.39	12	84647	
Lep72	lepidolite	0.0302	57.152	0.008	41.7	1.4	16	96908	
Lep82c	lepidolite	0.02202	68.34	0.18	86.20	0.89	9	96329	
Lep91	lepidolite	0.06194	55.163	0.018	28.32	0.17	21	85971	
Lep92	lepidolite	0.07247	56.23	0.35	28.76	0.24	21	85936	
Lep93	lepidolite	0.07468	56.66	0.059	36.50	0.29	17	91412	
Lep94	lepidolite	0.04503	52.341	0.001	19.02	0.17	29	85701	
Lep2017A2	lepidolite	0.23087	55.352	0.103	29.85	0.19	13	58742	One leachate divided into eight columns.
Lep2017B1			54.784	0.081	27.87	0.17	14	58504	
Lep2017C1			54.892	0.066	28.21	0.18	14	58514	
Lep2017C2			55.153	0.046	29.21	0.18	14	58526	
Lep2017D			53.974	0.063	24.91	0.15	16	58477	
Lep2017B1_2			55.110	0.063	29.03	0.18	14	58521	
Lep2017B2_2			54.739	0.043	27.70	0.17	14	58563	
Lep2017C1_2			54.768	0.054	27.81	0.18	14	58556	

The Siilinjärvi carbonatite was emplaced in the Late Archean. *In situ* Pb-Pb measurements gave a zircon age of 2594 ± 13 Ma (Rukhlov and Bell, 2010) with 1.8% discordance and an MSWD of 21. Both these findings indicate that the sample does not record a "geologically point-like" history, and that a systematic disturbance of the U-Pb system by far exceeds the measurement uncertainties. Indeed, the carbonatite was affected by post-emplacement regional metamorphism, dated with the lower discordia intercept at 1894 ± 78 Ma (Rukhlov and Bell, 2010). The undeformed appearance of the Siilinjärvi phlogopite (sample Si-102) in optical microscopy (see Fig.3) shows that mica (re-)crystallized during the metamorphic event. However, it is not known if the extent of the recrystallization was complete, nor if isotopic inheritance in relics was erased to 99.9 %. Due to its multiphase geological history, only limited attempts to date this sample were made after the initial analyses. A Rb-Sr age of 1869 ± 10 Ma (Fig.6a, Table 6) is indistinguishable from the lower discordia intercept. The K-Ca age of 1756 ± 112 Ma overlaps with the Rb-Sr age (Fig. 6b, Table 7).

Some Ca measurements showed a residual trend after the correction with the exponential fractionation law. As quantitatively discussed by Lehn and Jacobson (2015) for spiked samples and by Naumenko-Dèzes et al (2015) for standards, this residual trend is due to the incomplete fractionation correction provided by the first-order equations. The application of a second-order correction term (Caro et al., 2003; 2006) adapted to Ca (Naumenko-Dèzes et al., 2015) can in principle improve the first-order fractionation correction. However, due to very low amount of ^{42}Ca in analyzed samples, the uncertainty contributed by the second-order fractionation correction term was higher than the scatter of the points on the isochron. Due to such a residual trend observed for the $^{40}Ca/^{44}Ca$ ratio the uncertainties were calculated not as 2σ error, but as 2σ standard deviation (2SD) to cover the complete range of measured ratios. Samples PhB102aliq, PhB104aliq, Lep92 are affected the most by incomplete fractionation correction. This artefact was most pronounced for the samples with the smallest amounts of Ca (which required a more extensive filament depletion to reach an acceptable precision) and did not affect the standards, which were measured with higher filament loads.

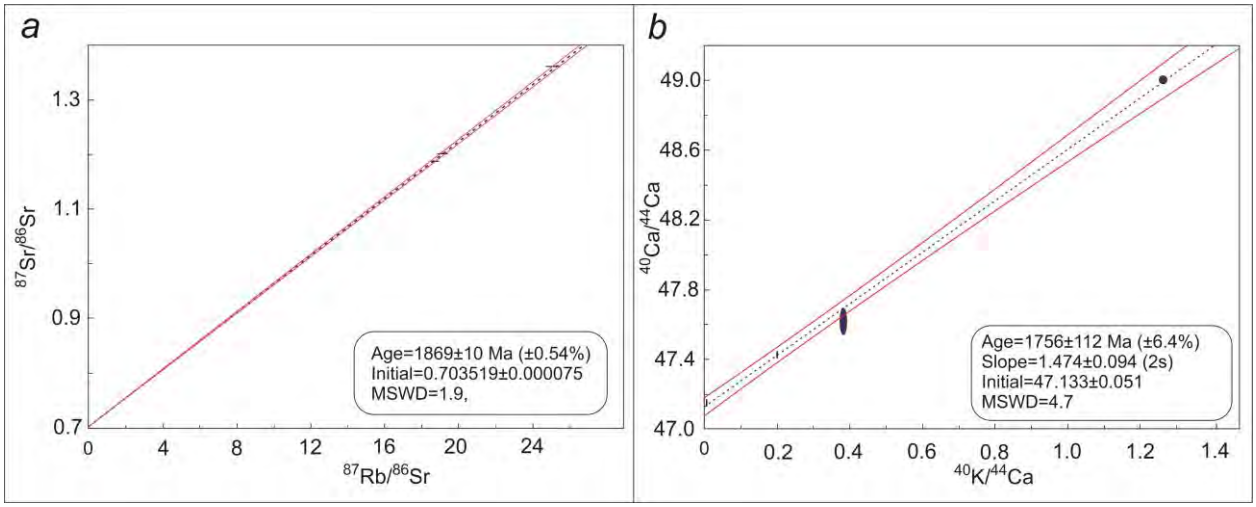

Fig.6. Isochron diagrams for the Siilinjärvi carbonatite: (*a*) Rb-Sr isochron for 3 phlogopites and a calcite. The symbols are enlarged on Y scale for visibility. The age is calculated with a decay constant $\lambda_{87} = (1.3972 \pm 0.0045)\times10^{-11}$ a^{-1} (Villa et al., 2015). (*b*) K-Ca isochron for three phlogopite and one calcite grain. The slope of 1.474 ± 0.094 corresponds to an age of 1756 ± 112 Ma with constants of Steiger and Jäger (1977).

391 Table 6. Rb-Sr results for the Siilinjärvi carbonatite. All uncertainties are given as 2 SE in-run uncertainty only.

Sample	Mineral	Mass (g)	$^{87}Sr/^{86}Sr$	2 SE	$^{87}Rb/^{86}Sr$	2 SE	Sr ppm	Rb ppm
Si5Bi	biotite	0.0064	6.549	0.406	223.1	13.9	6	305
Si61	biotite	0.0133	1.20055	0.00019	18.74	0.19	60	368
Si62	biotite	0.0078	1.18629	0.00011	18.35	0.16	58	350
Si8Bi1s	biotite	0.00295	1.35930	0.00036	24.59	0.32	42	336
Si8cal3s not spiked	calcite	0.0031	0.70352	0.00008	assumed = 0			

392

393 Table 7. K-Ca results for the Siilinjärvi carbonatite. All uncertainties are given as 2 SE in-run uncertainty only.

Sample	Mineral	Mass (g)	$^{40}Ca/^{44}Ca$	2 SE	$^{40}K/^{44}Ca$	2 SE	Ca ppm	K ppm
Si5Bi	biotite	0.00529	49.001	0.018	1.264	0.008	2212	463179
Si7Bi2	biotite	0.00459	47.608	0.060	0.379	0.007	1590	102576
Si7Bi1	biotite	0.00213	47.415	0.014	0.195	0.001	2526	84375
Si7cal1	calcite	0.01695	47.141	0.014	0.00000104	0.00000034	364447	65

394 # 4. Discussion

395

396 Despite the considerable effort spent in selecting suitable samples, that not all samples
397 chosen reflect geologically "point-like" events. The Siilinjärvi carbonatite underwent regional
398 metamorphism *ca*. 700 Ma after emplacement that affected the Rb-Sr and K-Ca systems in mica.
399 Because the system was not monogenetic this sample cannot be used for the decay constant
400 calibration.

401 The Rb-Sr age of the Rubikon lepidolite agrees with the literature U-Pb age of columbite,
402 indicating that the pegmatite may record a "point-like" geologic history. However, the large scatter
403 of the points along the K-Ca isochron prevents use of this sample for an intercomparison. The scatter
404 could be explained by an incomplete fractionation correction of the data with the conventional, first-
405 order exponential law. However, leaching experiments (Fig. 5b, green points; Fig. 5c) yielded a
406 data-set lying on a low dispersion isochron line, despite the fact that each individual point was
407 affected by an incomplete fractionation correction. It can be noted that the in-run fractionation of
408 these eight leach analyses was not as extreme as those of PhB102aliq, PhB104aliq, Lep92. It is
409 possible that the scatter of other points that were treated with HF is not due to the effect of
410 incomplete fractionation correction, but due to possible problems with incomplete digestion of
411 lepidolite with $HF+HNO_3$ acids, or (sub-percent) precipitation of CaF_2, or due to some other not yet
412 identified effect caused by the abundant Li and Al concentration in this sample. The isochron
413 defined by the leached aliquots gives an age of 481.3 ± 3.3 Ma (decay constants of Steiger and
414 Jäger, 1977). This K-Ca age is ca. 5 % younger than the U-Pb and Rb-Sr age of ca. 505 Ma (see
415 above).

416 The Phalaborwa complex fulfills all requirements for a geologically "point-like" event. It is
417 an intrusion that is well studied and has been dated multiple times with different methods (see Table
418 1). The uniform U-Pb age distribution for the whole complex shows that it crystallized and cooled
419 rapidly. The Rb-Sr age obtained in the present study is 2058.9 ± 5.2 Ma (2σ), which overlaps with
420 the U-Pb age. The K-Ca age calculated with the decay constants recommended in the past by IUGS

(Steiger and Jäger, 1977) is younger by approximately 1%. This confirms the suggestion made in the literature (*e.g.* Renne et al., 2010) that the four-decades-old IUGS recommendation is biased by ca. 1 %.

It should be pointed out that the Phalaborwa phlogopite, which looks pristine, coexists with minerals that have signs of alteration: diopside is serpentinized along cleavage planes, and apatite has discordant U-Pb systematics. Variations of element concentrations in phlogopite, which would diagnose alteration, have not been observed within the ca. 1 % resolution of the EPMA measurements.

4.1. ^{40}K decay constant

In order to translate the slope, *m*, of the K-Ca isochron into an age, the following equation must be solved:

$$t = (1/\lambda_{tot}) \times \ln (1 + (1/B_{Ca}) \times m) \qquad \text{Eq. 3}$$

where $B_{Ca} = \lambda_\beta/\lambda_{tot}$ is the branching ratio of the K-Ca decay. This equation has two unknowns, λ_{tot} and B_{Ca} and cannot be solved based on *m* of only one sample. It can however provide exclusion criteria for combinations of B_{Ca} and λ_{tot} that result in an inaccurate age for the analyzed sample. The age of the Phalaborwa complex calculated from the isochron slope (m = 1.878 ± 0.012), determined in the present study, with the constants from the most widely cited studies are presented in Table 8. It can be seen that most combinations give ages that are *ca*. 1 % too low; only the decay constants proposed by Min et al. (2000) are compatible with the U-Pb age, giving a K-Ca age that is higher by 10 ± 13 Ma.

Table 8. K-Ca age of the Phalaborwa phoscorite, calculated from the slope of the isochron in Fig. 4 for various combinations of the ^{40}K decay constants λ_β and λ_{tot} from the literature. The decay constants are taken as having zero uncertainty. The relative uncertainty of the slope is 0.64 %, which translates to an age uncertainty of 13.0 Ma for all entries. Units for the decay constants are 10^{-10} a^{-1}, units for ages are Ma. The branching ratio B_{Ca} is defined as $\lambda_{tot}/\lambda_\beta$. Most calculated ages are incompatible with the U-Pb age from Table 1, 2060.3 ± 0.4 Ma (Kumar et al., 2014).

λ_{tot}	λ_β	B_{Ca}	Age	Reference
5.543	4.962	0.8952	2040.0	Steiger and Jäger, 1977
5.549	4.974	0.8963	2036.2	Renne et al., 2010
5.531	4.955	0.8959	2043.6	Renne et al., 2011
5.543	4.947	0.8925	2043.5	Bé et al, 2014
5.541	4.942	0.8933	2045.2	λ_β from Kossert and Günther, 2004; B_{Ca} from Nägler and Villa, 2000
5.464	4.884	0.8939	2071.3	Min et al., 2000
5.484-5.498	*4.907-4.915*		*2060.4*	*"most reliable interval" (this study)*

As none of the decay constants from the literature are in full agreement with the results from the present study, an alternative way to constrain the most reliable "interval of reasonable values for the measurand" (JCGM, 2012, p. viii) is presented in Fig. 7. The age, the branching ratio of the K-Ca decay branch $B_{Ca} = \lambda\beta/\lambda_{tot}$ and the total decay constant are inversely proportional to each other; if λ_{tot} in the Eq. 3 is fixed to a certain published value, an age can be calculated that varies with B_{Ca} and family of parallel lines with negative slope is obtained. Fig. 7 shows three exemplary straight lines, corresponding to the combination of $\lambda\beta$ and λ_{tot} proposed by Steiger and Jäger (1977),

Min et al. (2000), and Renne et al. (2011). It is safe to restrict the infinity of straight lines only to those that intersect the horizontal band at 2060.3 ± 0.4 Ma (the U-Pb age of Phalaborwa) for B_{Ca} values between 0.8925 and 0.8963. The intersection with the horizontal band then gives the interval of the permissible λ_{tot} values: 5.484×10^{-10} a^{-1} < λ_{tot} < 5.498×10^{-10} a^{-1}. Note that this uncertainty interval does not correspond to a Gaussian distribution (as it is dominated by systematic artifacts of sample choice), therefore it would be incorrect to express it as a central value with associated standard deviation (JCGM, 2012).

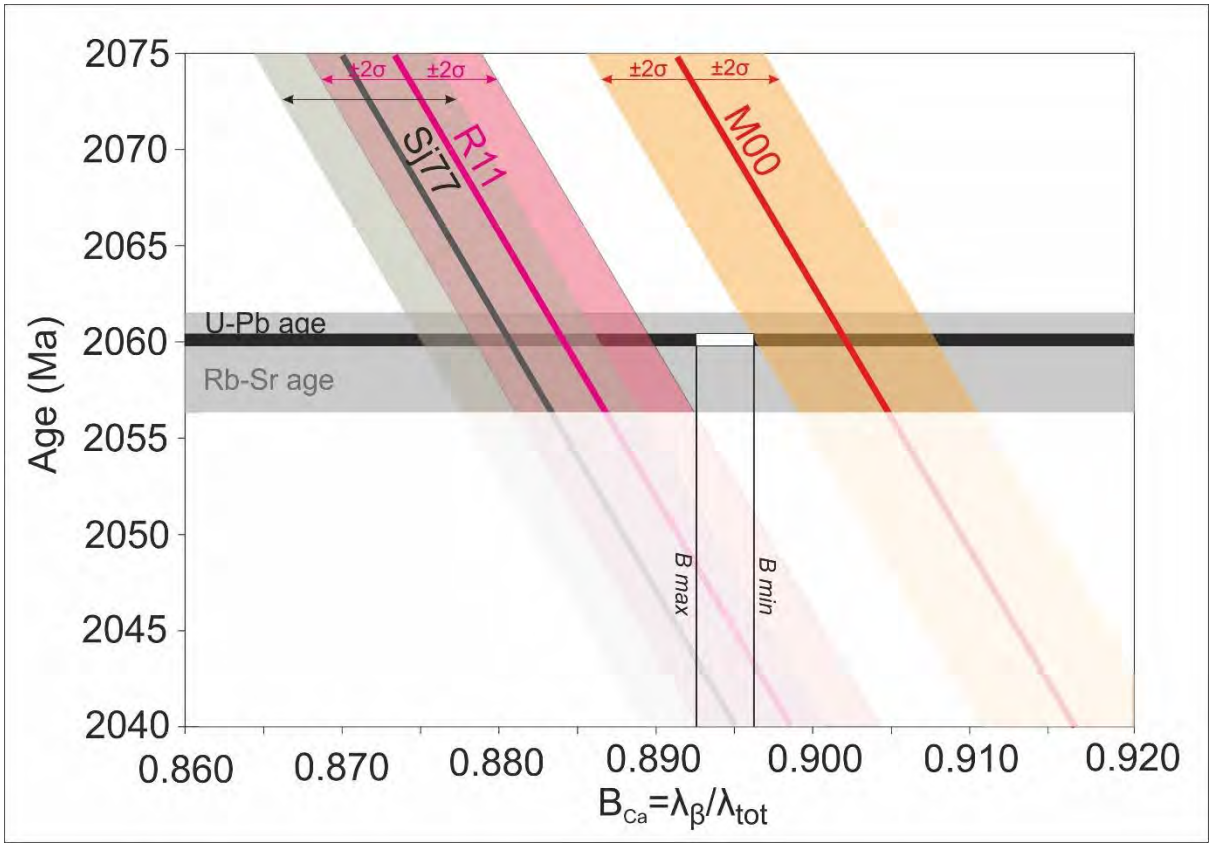

Fig. 7. Dependence of the K-Ca age on the choice of decay constants. The black and gray horizontal bands represent the reference U-Pb age and our Rb-Sr age of the complex, respectively. The vertical lines labeled B_{min} and B_{max} are the minimum and maximum literature values for B_{Ca}, as shown in Table 8. The inclined lines represent exemplary K-Ca ages calculated from the measured isochron slope (Fig. 4b); the width of the respective bands is the uncertainty of the K-Ca isochron (Fig. 4). The labels near the inclined lines refer to the source of the selected constants: SJ77, Steiger and Jäger (1977); M00, Min et al. (2000); R11, Renne et al. (2011). Other choices of constants from Table 8 are not plotted, as they lie between or very close to those by Steiger and Jäger (1977) and Renne et al. (2011). The total decay constant λ_{tot} and B_{Ca} are highly correlated, with a correlation coefficient practically equal to -1, i.e. the highest λ_{tot} corresponds to the leftmost inclined line and the lowest λ_{tot} to the rightmost line. The only lines that intersect the U-Pb age band in the x-axis interval [0.8925, 0.8963] are those with λ_{tot} in the interval [5.498×10^{-10} a^{-1}, 5.484×10^{-10} a^{-1}] (white rectangle). The corresponding λ_β is almost constant, as expected for a determination based on the K-Ca decay branch.

5. Conclusions

This study provides a narrow range for the ^{40}K decay constants based on intercalibration of the U-Pb, Rb-Sr and K-Ca decay systems for geological samples. The combination of petrologic screening with combined K-Ca–Rb-Sr dating on solution aliquots of the same mineral fragments ensured a reliable assessment of sample ideality. The single most important factor is the choice of natural samples whose internal heterogeneity (chemical and isotopic) must be less than 1%. In addition, the Rb-Sr and U-Pb age of minerals from the same geologic body have to agree within analytical uncertainty using the best determined decay constants. These criteria are only fulfilled by the sample from the Phalaborwa complex.

The 2058.9 ± 5.2 Ma Rb-Sr age of the Phalaborwa phoscorite phlogopite coincides with its U-Pb age (see Table 1). K-Ca dating of the phlogopite gave a statistically valid isochron with a slope of 1.878 ± 0.012. Use of the λ values of the current IUGS recommendation (Steiger and Jäger, 1977) yields an age of 2040 ± 13 Ma that is significantly lower than the Rb-Sr age of the same material and the U-Pb of coexisting baddeleyite. Forcing the K-Ca isochron slope to give an age coincident with the U-Pb and Rb-Sr ages gives one equation with two unknowns, $\lambda\beta$ and λ_{tot}. As the branching ratio of the K-Ca branch, B_{Ca}, has been estimated within a relatively narrow interval by all published references, $0.8925 < B_{Ca} < 0.8963$, it is possible to fix its value in this interval and explore the corresponding values of the total ^{40}K decay constant, λ_{tot}, that give a match with the U-Pb age. This gives the most reliable uncertainty interval ($k = 2$) as 5.484×10^{-10} $a^{-1} < \lambda_{tot} < 5.498 \times 10^{-10}$ a^{-1} for the total ^{40}K decay constant.

Acknowledgements

This work was sponsored by Swiss National Foundation grants 200021-131916 and 200020-153126. We are grateful to Dr. Beda Hofman (Naturhistorisches Museum der Burgergemeinde Bern) for providing the Rubikon lepidolite sample and to Prof. Keith Bell (Carleton University, Department of Earth Sciences) for several carbonatite samples, including Siilinjärvi. We are also thankful to the associate editor Dimitri Papanastassio and three anonymous reviewers for their suggestions and corrections. MND is thankful to Dr. Emelie Axelsson for her introduction to the Rb-Sr procedure.

References

Baadsgaard, H. (1987). Rb-Sr and K-Ca isotope systematics in minerals from potassium horizons in the prairie evaporite formation, Saskatchewan, Canada. *Chemical Geology (Isotope Geoscience Section)* **66**, 1-15.

Bé, M.-M., Christé, V., Dulieu C., Mougeot X., C., Browne, E., Chechev, V., Kuzmenko, N., Kondev F., Luca A., Galàn M., Nichols, A.L., Arinc A., Huang X. (2010). Table of Radionuclides, (Vol.5 - A=22 to 244 ed. *Bureau International des Poids et Mesures, Pavillon de Breteuil, F-92310 Sèvres*, p. 228.

Bé, M.-M., Dulieu, C., Mougeot, X., Kellett, M. (2014). HALF-LIVES. Table of recommended values, 2014 ed. *Bureau International des Poids et Mesures, Pavillion de Breteuil, F-92310 Sèvres,* p. 13.

Begemann, F., Ludwig, K.R., Lugmair, G.W., Min, K., Nyquist, L.E., Patchett, P.J., Renne, P.R., Shih, C.Y., Villa, I.M., Walker, R.J. (2010). Call for an improved set of decay constants for geochronological use. *Geochimica et Cosmochimica Acta* **65**, 111-121.

Caro, G., Bourdon, B., Birck, J.-L., Moorbath, S. (2006). High-precision $^{142}Nd/^{144}Nd$ measurements in terrestrial rocks: Constraints on the early differentiation of the Earth's mantle. *Geochimica et Cosmochimica Acta* **70**, 164-191.

Caro, G., Bourdon, B., Birck, J.-L., Moorbath, S. (2003). ^{146}Sm-^{142}Nd evidence from Isua metamorphosed sediments for early differentiation of the Earth's mantle. *Nature* **423**, 428-432.

Chu, Z.-y., Yang, Y.-h., Jinghui, G., Qiao, G.-s. (2011). Calculation methods for direct internal mass fractionation correction of spiked isotopic ratios from multi-collector mass spectrometric measurements. *International Journal of Mass Spectrometry* **299**, 87-93.

Davis, D. W., Gray, J., Gumming, G. l., and Baadsgaard, H. (1977). Determination of the ^{87}Rb decay constant. *Geochimica et Cosmochimica Acta* **41**, 1745–1749.

de Laeter, J.R., Böhlke, J.K., De Bièvre, P., Hidaka, H., Peiser, H.S., Rosman, K.J.R., Taylor, P.D.P. (2003). Atomic weights of the elements: Review 2000. *Pure and Applied Chemistry* **75**, 683-800.

Eriksson, S.C. (1984). Age of carbonatite and phoscorite magmatism of the Phalaborwa Complex (South Africa). *Chemical Geology* **46**, 291-299.

French, J.E., Heaman, L.M., Chacko, T. (2002). Feasibility of chemical U–Th–total Pb baddeleyite dating by electron microprobe. *Chemical Geology* **188**, 85-104.

Gopalan, K. (2008). Conjunctive K–Ca and Rb–Sr dating of glauconies. *Chemical Geology* **247**, 119-123.

Gopalan, K., Kumar, A. (2008). Phlogopite K-Ca dating of Narayanpet kimberlites, south India: Implications to the discordance between their Rb-Sr and Ar/Ar ages. *Precambrian Research* **167**, 377–382.

Heaman, L.M., LeCheminant, A.N. (1993). Geochemistry of Accessory Minerals Paragenesis and U-Pb systematics of baddeleyite (ZrO_2). *Chemical Geology* **110**, 95-126.

Heuser, A., Eisenhauer, A., Gussone, N., Bock, B., Hansen, B.T., Nägler, T.F. (2002). Measurement of calcium isotopes ($\delta^{44}Ca$) using a multicollector TIMS technique. *International Journal of Mass Spectrometry* **220**, 385-397.

Holmes, L., Cahen, L. (1956). Geochronologie Africanie. *Mémoires de la Classe de Sciences Naturelles et Médicales, Académie Royale des Sciences Coloniales (Bruxelles), Fasc* **1**, 169.

Horn, I., Rudnick, R.L., McDonough, W.F. (2000). Precise elemental and isotope ratio determination by simultaneous solution nebulization and laser ablation-ICP-MS: application to U–Pb geochronology. *Chemical Geology* **164**, 281-301.

Horwitz, E. P., Dietz, M. L., Chiarizia, R. (1992). The application of novel extraction chromatographic materials to the characterization of radioactive waste solutions. In Journal of Radioanalytical and Nuclear Chemistry **161**, 575–583.

JCGM (2012). Joint Committee for Guides in Metrology - The International Vocabulary of Metrology - Basic and General Concepts and Associated Terms, 3rd ed., JCGM 200:2012. JCGM.

Kossert, K., Gunther, E. (2004). LSC measurements of the half-life of ^{40}K. *Applied radiation and isotopes: including data, instrumentation and methods for use in agriculture, industry and medicine* **60**, 459-464.

Kumar, A., Nagaraju, E., Srinivasa Sarma, D., Davis, D.W. (2014). Precise Pb baddeleyite geochronology by the thermal extraction-thermal ionization mass spectrometry method. *Chemical Geology* **372**, 72-79.

Kwon, J., Min, K., Bickel, P.J., Renne, P.R. (2002). Statistical methods for jointly estimating the decay constant of ^{40}K and the age of a dating standard. *Mathematical Geology* **34**, 457-474.

Lehn G. O., Jacobson A. D. (2015) Optimization of a ^{48}Ca-^{43}Ca double-spike MC-TIMS method for measuring Ca isotope ratios ($\delta^{44/40}Ca$ and $\delta^{44/42}Ca$): limitations from filament reservoir mixing. J. Anal. At. Spectrom. 30, 1571–1581. http://dx.doi.org/10.1039/C4JA00412D.

Ludwig, K.R. (2012). Isoplot3_75, A Geochronological Toolkit tor Microsoft Excel, 3.75 ed, Berkley Geochronology Center

Melcher, F., Graupner, T., Gäbler, H.-E., Sitnikova, M., Henjes-Kunst, F., Oberthür, T., Gerdes, A., Dewaele, S. (2015). Tantalum-(niobium-tin) mineralisation in African pegmatites and rare metal granites: Constraints from Ta-Nb oxide mineralogy, geochemistry and U-Pb geochronology. *Ore Geology Reviews* **64**, 667-719.

Miiller A. P. (2006). Development of argon isotope reference standards for the U.S. Geological Survey, *Journal of Research of the National Institute of Standards and Technology* **111**(5), 335-360.

Min, K., Mundil, R., Renne, P.R., Ludwig, K.R. (2000). A test for systematic errors in Ar-Ar geochronology through comparison with U-Pb analysis of a 1.1-Ga rhyolite. *Geochimica et Cosmochimica Acta* **64**, 73-98.

Morgan L.E., Postma O., Kuiper K.F., Mark D.F., Plas W.v.d., Davidson S., Perkin M., Villa I.M., Wijbrans J.R. (2011). A metrological approach to measuring ^{40}Ar* concentrations in K-Ar and ^{40}Ar/^{39}Ar mineral standards. *Geochemistry Geophysics Geosystems*, Paper #2011GC003719, doi: 10.1029/2011GC003719

Mougeot X., Helmer R.G. (2009). ^{40}K - Comments on evaluation of decay data. Gamma and alpha spectrometry on-line library. Laboratoire National Henri Becquerel. http://www.nucleide.org/Laraweb/

Nägler T.F., Kamber B.S. (1996). A new Silicate dissolution procedure for isotope studies on garnet and other rock forming minerals. Schweizerische. *Mineralogische und Petrographische Mitteilungen* **76**, 75-80.

Nägler, T.F., Villa, I.M. (2000). In pursuit of the ^{40}K branching ratios: K-Ca and ^{39}Ar-^{40}Ar dating of gem silicates. *Chemical Geology* **169**, 5-16.

Naumenko-Dèzes, M.O., Bouman, C., Nägler, T.F., Mezger, K., Villa, I.M. (2015). TIMS measurements of full range of natural Ca isotopes with internally consistent fractionation correction. *International Journal of Mass Spectrometry* **387**, 60-68.

Naumenko, M.O., Mezger, K., Nägler, T.F., Villa, I.M. (2013). High precision determination of the terrestrial ^{40}K abundance. *Geochimica et Cosmochimica Acta* **122**, 353-362.

Nebel, O., Scherer, E.E., Mezger, K. (2011). Evaluation of the ^{87}Rb decay constant by age comparison against the U–Pb system. *Earth and Planetary Science Letters* **301**, 1-8.

Reischmann, T. (1995). Precise U/Pb age determination with baddeleyite (ZrO_2), a case study from the Phalaborwa igneous complex, South Africa. *South African Journal of Geology* **98**, 1-4.

Renne, P.R., Balco, G., Ludwig, K.R., Mundil, R., Min, K. (2011). Response to the comment by W.H. Schwarz et al. on "Joint determination of ^{40}K decay constants and ^{40}Ar*/^{40}K for the Fish Canyon sanidine standard, and improved accuracy for ^{40}Ar/^{39}Ar geochronology" by P.R. Renne et al. (2010). *Geochimica et Cosmochimica Acta* **75**, 5097-5100.

Renne, P.R., Mundil, R., Balco, G., Min, K., Ludwig, K.R. (2010). Joint determination of ^{40}K decay constants and ^{40}Ar*/^{40}K for the Fish Canyon sanidine standard, and improved accuracy for ^{40}Ar/^{39}Ar geochronology. *Geochimica et Cosmochimica Acta* **74**, 5349-5367.

Rotenberg E., Davis D.W., Amelin Y., Ghosh S., Bergquist B.A. (2012) Determination of the decay-constant of ^{87}Rb by laboratory accumulation of ^{87}Sr. *Geochim. Cosmochim. Acta* **85**, 41-57.

Rukhlov, A.S., Bell, K. (2010). Geochronology of carbonatites from the Canadian and Baltic Shields, and the Canadian Cordillera: clues to mantle evolution. *Mineralogy and Petrology* **98**, 11-54.

Russell, W.A., Papanastassiou, D.A., Tombrello, T.A. (1978) Ca isotope fractionation on the Earth and other solar system materials. Geochimica et Cosmochimica Acta **42**, 1075-1090.

Shih C. Y., Nyquist L. E. and Wiesmann H. (1993). K-Ca chronology of lunar granites. *Geochim. Cosmochim. Acta* **57**, 4827–4841.

Steiger, R.H., Jäger, E. (1977). Subcommission on geochronology: convention on the use of decay constants in geo- and cosmochronology. *Earth and Planetary Science Letters* **36**, 359-362.

Villa I.M. (2016). Diffusion in mineral geochronometers: present and absent. *Chemical Geology* **420**, 1-10.

Villa I.M., Ruggieri G., Puxeddu M., Bertini G. (2006). Geochronology and isotope transport systematics in a subsurface granite from the Larderello-Travale geothermal system (Italy). *Journal of Volcanology and Geothermal Research* **152**, 20-50.

Villa, I.M., De Bièvre, P., Holden, N.E., Renne, P.R. (2015). IUPAC-IUGS recommendation on the half life of ^{87}Rb. *Geochimica et Cosmochimica Acta* **164**, 382-385.

Wingate, M.T.D., Compston, W. (2000). Crystal orientation effects during ion microprobe U–Pb analysis of baddeleyite. *Chemical Geology* **168**, 75-97.

607 Wu, F.-Y., Yang, Y.-H., Li, Q.-L., Mitchell, R.H., Dawson, J.B., Brandl, G., Yuhara, M. (2011). In situ
608 determination of U-Pb ages and S-Nd-Hf isotopic constraints on the petrogenesis of the Phalaborwa carbonatite
609 Complex, South Africa. *Lithos* **127**, 309-322.

610 Yuhara, M., Hirahara, Y., Nishi, N., Kagami, H. (2005). Rb-Sr, Sm-Nd ages of the Phalaborwa Carbonatite
611 Complex, South Africa. *Polar Geoscience* **18**, 101-113.

612

Appendix 1

Click here to download Appendix: Appendix_1_K_Ar_age_monitors_Naumenko_2017.pdf

Appendix 2

Click here to download Appendix: Appendix_2_EMPA_Naumenko_2017.xlsx

Appendix 3

Click here to download Appendix: Appendix_3_K_Ca_sample_dissolution_Naumenko_2017.xlsx

Appendix 4

Click here to download Appendix: Appendix_4_Fractionatio_ correction_Naumenko_2017.pdf

***Manuscript (doc)**

Click here to download Source or Other Companion File: NaumenkoGCA07.07.2017.docx

Appendix 1 (doc)

Click here to download Source or Other Companion File: Appendix_1_K_Ar_age_monitors_Naumenko_2017.doc

Appendix 4 (doc)

Click here to download Source or Other Companion File: Appendix_4_Fractionatio_ correction_Naumenko_2017.docx